PERGAMON

Electrochimica Acta 45 (2000) 2595–2609

ELECTROCHIMICA Acta

www.elsevier.nl/locate/electacta

Mathematical modeling of secondary lithium batteries

Gerardine G. Botte, Venkat R. Subramanian, Ralph E. White *

Department of Chemical Engineering, Center for Electrochemical Engineering, University of South Carolina, Columbia, SC 29208, USA

Papers received in Newcastle, 20 December 1999

Abstract

Modeling of secondary lithium batteries is reviewed in this paper. The models available to simulate the electrochemical and thermal behavior of secondary lithium batteries are discussed considering not only their electrochemical representation (transport phenomena and thermodynamics of the system), but also the mathematical techniques that have been used for solving the equations. A brief review of the governing equations for porous electrodes, and methods for solving these equations is also given. © 2000 Elsevier Science Ltd. All rights reserved.

Keywords: Secondary lithium batteries; Intercalation; Electrochemical modeling; Thermal modeling

1. Introduction

Mathematical modeling of batteries requires specification of the dependent variables of interest (e.g. concentration of electrolyte), the governing equations for these variables, the initial and boundary conditions for these variables, and a method of solution of the resulting system of equations. We present here a brief review of the governing equations for porous electrodes, methods for solving these equations, and some of the mathematical models that have been presented for secondary lithium batteries.

Mathematical modeling of electrochemical systems that include porous electrodes is based on governing equations for the dependent variables of interest. Bird et al. [1] present a through review of many equations similar to those needed for porous electrodes. Newman [2] presents many of these equations as applied to electrochemical systems. Newman and Tiedemann [3] present governing equations for porous electrodes. The details associated with the derivation of these porous electrode equations are given by Dunning [4] and Trainham [5]. De Vidts and White [6] also present equations for porous electrodes which they derived by using a volume-averaging technique. Some of the equations derived by De Vidts and White [6] include terms not included in the equations derived by others [3–5]; however, their [6] equations simplify to those presented by Newman and Tiedemann [3] under specific assumptions [6]. Similar equations to those presented by De Vidts and White [6] where presented by earlier Prins-Jansen et al. [7]. Wang et al. [8] developed a micro-macroscopic coupled model, that incorporates solid-state physics of electrode materials, interface morphology and chemistry for advance batteries and fuel cells using the volume-averaging technique.

Bernardi et al. [9] present a general energy balance for battery systems. Rao and Newman [10] extended the same equation to account for the energy balance in insertion battery systems. Botte et al. [11] extended Rao and Newman's energy balance [10] to incorporate the effect of side reactions in the thermal behavior of a cell. Botte et al. [11] presented details of transforming the general energy equation (Eq. (3) of Ref. [11]) to the applied form of the equation (Eq. (7) of Ref. [11]).

Once the governing equations have been determined for the dependent variables of interest, one should simplify these equations as needed to provide as simple a model as possible to answer to questions posed.

---

* Corresponding author. Tel.: + 1-803-7773270; fax: + 1-803-7778265.

E-mail address: rew@sc.edu (R.E. White)

0013-4686/00/$ - see front matter © 2000 Elsevier Science Ltd. All rights reserved.

PII: S0013-4686(00)00340-6

However, one should check carefully all of the assumptions made. Sometimes, assumptions are made implicitly and, consequently, the final results do not make physical sense. For example, the final mass of electrolyte should not be larger than the initial mass of electrolyte after simulating a discharge. This type of result can occur when volume changes occur in the system due to chemical reactions. Jain and Weidner [12] present examples of these problems and show how to modify the material balance of a one-dimensional porous electrode to account for volume changes and to account for an inflow of electrolyte from the header of the battery into the active pores of the electrode. The authors [12] show how the assumption of volume conservation is often inadvertently incorporated into models. This problem can be avoided by going carefully from general equations to simplified ones.

Once the governing equations have been simplified, they have to be solved. The first thing to do is to look for an analytical solution [13,14]. Unfortunately, analytical solutions are not available for most of cases of interest. Nevertheless, they are the best if available or can be obtained. The reason for this is that analytical solutions are continuous in the independent variables, and show explicitly how the parameters of the system are involved. Also, analytical solutions give much insight into a system, which is one of the primary objectives of modeling.

Classical analytical techniques are: Laplace transformation, separation of variables, conformal mapping, method of images, Green's function, perturbation, etc. However, analytical techniques are specific to the system, geometry and boundary conditions. Often times, analytical solutions involve integrals, eigenvalues, etc. which must be evaluated or obtained numerically.

Usually, complicated models must be solved using numerical techniques. Numerical techniques are very general, and valid for most models. The speed and accuracy of the technique depends upon the technique, system, complexity of boundary conditions, etc. The most common numerical techniques for modeling electrochemical systems are: the finite difference method (FDM), the control volume formulation (CVF), and the finite element method (FEM).

The FDM has been used extensively [15–34] due to its simplicity and accuracy. However, it has been pointed out that mass is conserved in the FDM only in the limit when the grid spacing size goes to zero [35,36]. To avoid this discrepancy, some authors [35–43] have used the control volume formulation (CVF) also known as finite volume method. Botte et al. [44] have shown that the CVF performs better than the FDM only for a boundary value problem (BVP) in which the two boundary conditions are given as fluxes. In all other cases, the FDM is more accurate than the CVF for a small number of nodes especially when interface boundary conditions are presented in the system [44]. Botte and White [45] have shown that the false boundary method (FBM) can be used to obtain mass conservation in boundary value problems in which the two boundary conditions are given as fluxes; however, when only one of the boundary conditions is given as a flux, the FDM is more accurate for one flux boundary condition than the FBM for a small number of nodes.

The finite element method (FEM) provides an alternative to model systems with irregular geometry, unusual boundary conditions, or heterogeneous composition [46]. However, the FEM is more difficult to program than the FDM, CVF, and/or FBM.

The programming code/language should be chosen according to the degree of difficulty of the models. Analytical solutions once found in the literature or derived for a new system can be programmed in a symbolic language like Maple, Mathcad, Mathematica or in FORTRAN or C++.

Analytical solutions are usually restricted to linear equations. Often times, even analytical solutions for linear equations with linear boundary conditions involve eigenvalues, which are to be found by solving non-linear equations. For non-linear equations, one might attempt to get series solutions using perturbation [47] or other symbolic techniques [48] which enable one to solve non-linear equations symbolically with the parameters in the final solution as in analytical solutions. A semi-analytical (or analytical method of lines) technique [19–22,49,50], which is analytical in one of the independent variables and numerical in the other is found to be more efficient than both analytical and completely numerical techniques for many problems. The use of the exponential matrix for solving partial differential equations (PDEs) was mentioned by Smith et al. [49] in 1970 and used in 1987 by De Vidts and White [19] to solve the diffusion equations. Haran and White [20], extended the same technique to non-linear PDEs by using Maple. Subramanian and White [21,22] extended the same technique to the Laplace equation for solving current density and potential distributions in electrochemical systems. Other programs to solve PDEs have been developed by the authors using Maple [50]. As mentioned earlier, there are other software available for programming mathematical applications such as Mathcad [51] and Mathematica [52]. All of this software (Maple, Mathcad and Mathematica) allows numerical, symbolic and graphical mathematical computations.

Many numerical techniques have been developed for solving non-linear equations. The simplest and still most commonly used technique is based on finite differences. Newman's BAND subroutine [2] has been used for electrochemical systems for more than three decades. Software like Maple and Mathematica can be used for determining the Jacobians and the associated

FORTRAN code for use with the BAND subroutine. White [23] provided a derivation of the BAND subroutine and extended the same for linearizing non-linear finite difference expressions. Van Zee et al. [24], extended Newman's BAND subroutine to solve coupled, non-linear partial differential equations by using the implicit alternating direction technique (IAD). Nguyen and White [25] presented a finite difference procedure for solving coupled, nonlinear elliptic partial differential equations. They showed how their method was faster than the IAD scheme suggested by Van Zee et al. [24] Fedkiw [26] used a collocation-finite difference procedure for solving elliptic PDEs. Curtis et al. [27] compared Newman's technique with deBoor's algorithm [53]. They showed that Newman's BAND subroutine in some cases returns incorrectly a message 'determinant equals zero'. They discussed how this 'zero determinant problem' can be avoided. Preisig and White [28] provided an alternate simple solver for nonlinear two-point BVPs where they used an algebraic manipulator (MATLAB) for generating the Jacobians. Matlosz and Newman [29] solved one-dimensional BVPs using BandAid. Van Zee et al. [30] presented a pentadiagonal BAND subroutine for solving BVPs, which is accurate to the order $(\Delta x)^4$. Kimble and White [31] presented an implicit five-point finite difference method for solving parabolic partial differential equations. Their method is accurate to the order $(\Delta t)^4 + (\Delta x)^4$. They obtained high accuracy with only six nodal points in each dimension. Fan and White [32], modified Newman's BAND subroutine to multi-region systems containing interior boundaries, they called the new subroutine MBAND. They showed that their technique is faster than the pentadiagonal BAND developed by Van Zee et al. [30] Their technique is capable of handling multiple regions with discontinuity in the interfaces. Fan and White [33] optimized a pentadiagonal version of BAND. Mao and White [34] presented a finite difference method for pseudo-two-dimensional BVPs and showed that their method was superior to the previously existing techniques. Subramanian and White have developed a Maple program for generating Jacobians for any order of accuracy.

The trend in numerical solution of mathematical models in electrochemical systems is to the use of commercially available software such as PDE2D [54], FLUENT CFD [55], DASSL [56–60], etc. PDE2D [54] is a numerical PDE solver based on finite elements using Hermite cubic basis functions. The main advantage of PDE2D is that one can integrate the dependent variables over a region as well as along a boundary. It can also handle curved domains. PDE2D can be used to solve three-dimensional BVPs of any kind and geometry. FLUENT CFD [55] is a computational fluid dynamics software package that allows solving momentum, mass and energy balances using the control volume technique. The software is user friendly and allows automatic generation of the mesh. DASSL [56–60] is a robust package for solving equations and one needs not to calculate the Jacobians as required with BAND [2]. DASSL finds the Jacobians itself and uses an optimum step size in time for integration and is adaptive in time. There are other differential equation solvers available in the market that can be used in modeling of electrochemical systems (e.g. Diffpack [61]). FWEB [62] has also been used for literate programming [56]. FWEB enables one to build a documented program that can be easily understood. In addition, FWEB can be used with several of the more important compiled languages: C, C + +, FORTRAN (both F77 and F90), RATFOR, and TeX [62]. The fact that this software is able to recognize the syntax of different languages is an important feature because some languages are much easier to use than others (also some subroutines are already time tested in different languages). Therefore, FWEB may play an important role by enabling on the ability to mix different languages in the same program, which may reduce the time of programming.

The last step but not the least important in modeling a system is to measure, search, or estimate the properties and parameters to use in the model. The model will only be as good as the data used. The measurement of transport properties, kinetics parameters, and physical properties is not an easy job, especially for properties in the solid phase (electrodes). For this purpose, molecular simulations are very important because they allow to understand the details of the process and to provide physical properties that can be used in the macroscopic model.

Some readers may want to review the work being done by Professor Compton's research group [63]. They work on computational electrochemistry (especially electrode/electrolyte interfaces) and on modeling and designing the experimental techniques to understand the electrochemical reactions taking place at the electrode surfaces. Also, one may want to review the work of Bieniasz [64] who also works on modeling of electrochemical systems.

In the next section we describe the topics discussed above applied to secondary lithium batteries as an example of modeling electrochemical systems. Below is presented a discussion in the techniques used for the estimation of properties and parameters used in the modeling of these batteries.

Transport properties, kinetics parameters, and physical properties for lithium batteries have been reported for several authors [65–72]; however, there is still a lot of work to do in this area. Doyle [73] gives a summary of open circuit potential data for different electrode materials use in secondary lithium batteries. Hong et al. [74] have used calorimetric techniques and the potentiometric method to measure the entropy of reaction term during the discharge of a Sony-type US 18650 cell. This entropy of reaction term is required for the thermal modeling of the cell. Maleki et al. [75] measured thermal property data for the Sony US-18650 lithium-ion battery and its components. They found that the heat capacity of the battery depends on its state of charge and they associated this behavior with the structural changes that take place in the anode and cathode during their lithiation and delithiation [75]. The authors [75] also measured the thermal conductivities of this system: cross-plane thermal conductivity and in-plane thermal conductivity. They found differences in the values of the cross-plane and in-plane thermal conductivities and they attributed those to the orientation of particles during the formation of thin electrode layers and to the presence of metallic current collectors. These differences in the cross-plane and in-plane thermal conductivities may be important for modeling the thermal behavior of the battery in more than one dimension.

Some authors [76–81] have used first principles, molecular simulations and computational chemistry to have a better understanding of the lithium batteries (e.g. lithiation of the electrodes) and to calculate physical properties (mobility of lithium in different solvents, diffusion coefficients of lithium in different solvents, etc.). Reimers [82] described how first principle calculations can aid in the design of lithium ion batteries. He states that first principles can be used to calculate voltage curves of electrode materials in lithium-ion cells. First principles calculations can help understanding physical situations such as the state of charge dependence of the heat capacity of the cell described by Maleki [75]. Marquez et al. [79] used first principles calculations to model graphite in the presence of tetrahydrofuran solvent (THF). They addressed the structural changes that are produced in the graphite by the presence of lithium and solvent. The trend is to combine first principle calculations and molecular simulations with experimental work to understand the basis of the materials (physical and transport properties) used in secondary lithium batteries. It is worth mentioning that experiments would not be substituted by first principles calculations and molecular modeling but the number of them would be reduced with the aid of these calculations.

2. Secondary lithium batteries

Mathematical modeling of secondary lithium batteries begins by drawing a schematic of the cell. Fig. 1a presents a schematic representation of a lithium-ion cell sandwich (according to Hossain's classification [83]). The negative and the positive electrodes are composite materials, and they are represented as spherical particles in Fig. 1a. During a discharge process the lithium ions de-intercalate from the negative electrode, diffuse through the separator/electrolyte and intercalate into the positive electrode. The opposite process takes place during charge. Fig. 1b presents a schematic representation of a liquid organic electrolyte cell with a solid lithium foil serving as the negative electrode (according to Hossain's classification [83]). The insertion and de-insertion process in the particles used to make the porous electrodes shown in Fig. 1a and b can be described by [84]

$$\mathrm{Li}^+ + \mathrm{e}^- + \theta_s \rightleftharpoons \mathrm{Li} - \theta_s \tag{1}$$

Several models [11,56,72,84–109] have been presented for studying the behavior of secondary lithium cells. These models can be divided in two types: (1) General models [56,72,84–101] that cover modeling of the electrochemical performance of the cells, and (2) Thermal models [11,102–109] that cover the thermal performance of the cell.

2.1. General models

Some models for secondary lithium batteries [85–89] have been developed using simplified equations for different limiting cases that allow obtaining analytical solutions for the system. A one-dimensional cell sandwich is typically used (as shown in Fig. 1(a) [89] and (b) [85–88]), where the transport properties are assumed to be independent of the concentration and dilute solution theory for a binary electrolyte is used. Atlung et al. [85] developed analytical solutions for a solid-diffusion phase limitation in a liquid–organic electrolyte cell ($\mathrm{Li/LiClO_4}$–$\mathrm{PC/TiS_2}$). Their expressions [85] allow evaluating different shapes of particles (plane sheet, cylinders, and spheres), and their assumptions are similar to those used by Doyle and Newman [86]. Atlung et al. [85] defined some dimensionless parameters that together with the shape of the particle fully describe the behavior of the cathode under a constant current load.

Doyle and Newman [86] developed analytical solutions for three different limiting cases: solution-phase diffusion limitations, solid-phase diffusion limitations, and ohmically dominated reaction zone model. They modeled a polymer electrolyte cell (Li/solid polymer electrolyte/$\mathrm{Li_yMn_2O_4}$). In the solution-phase limitation case it was assumed that the kinetic resistance dominates the ohmic resistance, therefore, a uniform current distribution can be expected [2]. They used separation of variables to obtain the solution of the system of equations. It is worth mentioning that a steady state solution cannot be obtained for their Eqs. (9)–(15), in the way suggested in their paper [86]. That is, a steady state solution for two flux boundary conditions cannot be obtained directly using the method described by them. The way to obtain this kind of solution is by solving the unsteady state problem and making the two fluxes at the boundary conditions the same (steady state condition: flux in equal to flux out). These kind of differential equations can be solved by using the technique proposed by Subramanian and White [110].

If the discharge rate is high, it is possible to have solid-diffusion limitations, a measure of the importance of solid-phase diffusion limitations can be found from [84,86,90]

$$S_s = \frac{R_s^2\, I}{D_s F(1-\varepsilon)c_t\, L_e} \tag{2}$$

If $S_s < < 1$, diffusion in the solid phase is fast. This criterion is very useful because it provides a means for estimating the solid diffusion effect of different materials.

If the transference number is close to one, the concentration gradients can be neglected in a cell and an ohmically-dominated reaction zone model applies [86,87]. Atlung et al. [88] obtained an approximate solution for this limiting case; however, they considered a fixed position for the boundary conditions, while Doyle and Newman [86,87] incorporated the effect of a moving zone boundary condition to account for the displacement of the reaction zone. The work by Atlung et al. [88] is valid during the initial transient period, that is, until the capacity at the front of the electrode is exhausted, while the work by Doyle and Newman [86,87] is valid for long times and for small values of the slope of the open circuit potential (assumed to be a linear function of the lithium intercalation fraction). More details about the applicability of the reaction-zone model (moving zone boundary condition) can be obtained by analyzing Eq. (22) of Ref. [87].

Darling and Newman [89] developed approximate solutions for the short time behavior of a one dimensional lithium-ion cell. Their approximate analytical solutions are useful for evaluating the reaction-rate

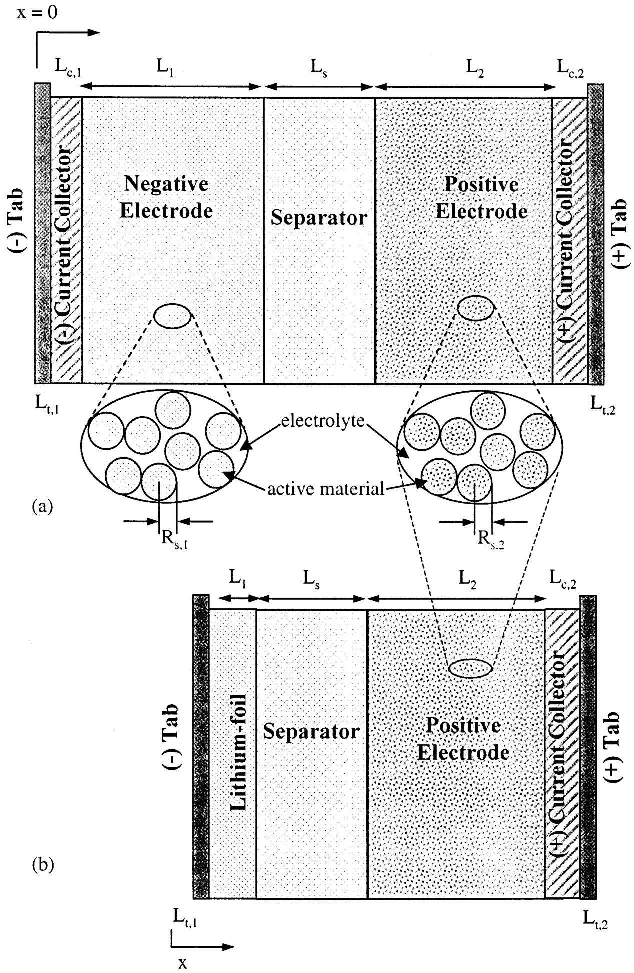

Fig. 1. Schematic cell sandwich representation of a secondary lithium battery. (a) Lithium ion cell and (b) liquid orgainc electrolyte cell (solid lithium foil serving as the negative electrode). The active material is represented as spherical particles.

distribution in composite electrodes like those shown in Fig. 1. The Laplace transform method was used to develop the analytical solutions. They used numerical techniques [111,112] for inverting the variables in the Laplace transform domain. Despite the simplicity of these models [85–89], they have some features that are worth mentioning: they provide an approximate response of the battery under certain limiting cases, they use a small number of parameters (more complete models require a large number of parameters), they provide dimensionless terms that allow obtaining expressions to identify limiting cases, they can be used to estimate transport and kinetics properties and for a preliminary design of the system, etc.

The intercalation of lithium in the electrode has been modeled as a solid diffusion process by many authors [56,84–99]. This approach consists of solving the diffusion equation in a spherical particle

$$\frac{\partial c_s}{\partial t} = D_s\left[\frac{1}{r^2}\frac{\partial}{\partial r}\left(r^2\frac{\partial c_s}{\partial r}\right)\right] \tag{3}$$

where c_s is the concentration of lithium inside a spherical electrode particle. The diffusion coefficient D_s is assumed to be constant. The boundary conditions are

$$\frac{\partial c_s}{\partial r}(0, t) = 0 \tag{4}$$

and

$$D_s\frac{\partial c_s}{\partial r}(R_s, t) = -j_n \tag{5}$$

where j_n is the pore wall flux of Li^+ at the surface of the electrode particle and R_s is the radius of the particle. The battery is usually fully charged initially

$$c_s(r, 0) = c_s^0 \tag{6}$$

where c_s^0 is the initial concentration of Li^+ in the particle.

Eq. (5) is used as the boundary condition at the surface of the particle for many models [56,84–90,93–99]; others use an equilibrium condition at the electrode surface (i.e. no kinetics resistance for charge transfer at the particle surface) [91,92,97]:

$$\phi_1 - \phi_2 = (\phi_1 - \phi_2)^\theta + \frac{RT}{F}\left[\ln\left(\frac{c_t - c_s^*}{c_s^*}\right) + \ln\left(\frac{c_+}{c^0}\right) - f(c_s^*/c_t) - 0.5\right] \tag{7}$$

instead of Eq. (5). Where $(\phi_1 - \phi_2)^\theta$ and f are characteristic constants of the electrode material. Applying Eq. (7) implies that the insertion process is equivalent to an adsorption process with a linear interaction term (Frumkin isotherm) [91].

Verbrugge and Koch [100] extended the above treatment of diffusion of lithium ions in a solid by using the gradient of the chemical potential as the driving force, instead of the gradient of the concentration; consequently, their governing equation for the insertion process assuming a constant diffusion coefficient is given by

$$\frac{\partial \theta_I}{\partial t} = D_I\nabla\cdot\left[\left(1 + \frac{d\ \ln\gamma_I}{d\ \ln\theta_I}\right)\nabla\theta_I\right] \tag{8}$$

where θ_I represents the fraction of sites occupied by lithium ions in the electrode particle. To obtain the dependence of the activity coefficient (γ_I) on the occupancy fraction (θ_I), they expressed the excess free energy (G^E) as a series expansion of the occupancy fraction (θ_I), as was initially proposed by Wohl [113]

$$G^E = \sum_{k=2}^{N}\Omega_k\theta_I^k \tag{9}$$

and used open circuit potential data for a single particle as a function of the intercalation fraction to obtain the interaction parameters (Ω_k) by using a least square method. Once the Ω_k are known, activity coefficients can be calculated and Eq. (8) can be solved with similar boundary conditions and initial conditions as those given by Eqs. (4) to (6). In their case the boundary condition at the surface of the particle includes the effect of the activity coefficients (see their Eq. (12)). They used partially graphitic carbon fibers for their experiments and found the quantity $(1 + d\ \ln\gamma_I/d\ \ln\theta_I)$ to be a strong function of concentration. Their theoretical calculations show good agreement with seven different experimental data sets. These results are significant and indicate that using a concentration gradient as the driving force for this material is not appropriate, because the activity coefficients are far from ideal values. Experiments like those done by Verbrugge and Koch [100] should be done with other materials that are used to make anodes and cathodes in lithium batteries to determine the importance of the interactions. If the interactions for these materials are found to be significant, the diffusion model would not be a realistic representation for the intercalation process in the electrodes. Uchida et al. [114] have used microvoltammetric techniques to investigate the solid-state electrochemistry of $LiCoO_2$ and spinel-related manganese oxides.

Recently, Verbrugge and Koch [72] extended their approach of using the chemical potential driving force given in Eq. (8) (but D_I was not assumed to be constant), to measure the variation of the diffusion coefficient in the solid phase with the intercalation fraction in a porous electrode containing poly(acrylonitrile) fibers. They worked in the range where the diffusion in the solid phase is the limiting process (that is, $S_s > > 1$, see Eq. (2) and obtain an analytical solution for short times using perturbation techniques.

West et al. [91] modeled a liquid organic electrolyte cell (Li/LiClO$_4$–PC/TiS$_2$) using dilute solution theory [2] for the transport in the electrolyte phase (including diffusion and migration). They [91] treated the transport in the electrolyte as a one-dimensional problem. Their model includes lithium foil as the negative electrode and TiS$_2$ as the positive electrode. Their equations can be summarized by

$$\frac{\partial c_+}{\partial t} = D_-\left[\frac{\partial^2 c_+}{\partial x^2} - \frac{F}{RT}\left(\frac{\partial c_+(x)}{\partial x}\frac{\partial \phi_2(x)}{\partial x} + c_+(x)\frac{\partial^2 \phi_2(x)}{\partial^2 x}\right)\right] \tag{10}$$

$$\frac{\partial c_+}{\partial t} = D_+\left[\frac{\partial^2 c_+}{\partial x^2} - \frac{F}{RT}\left(\frac{\partial c_+(x)}{\partial x}\frac{\partial \phi_2(x)}{\partial x} + c_+(x)\frac{\partial^2 \phi_2(x)}{\partial^2 x}\right)\right] + \frac{i_2(x)\, g}{F} \tag{11}$$

for the anions and cations, respectively in the electrolyte phase. With the boundary conditions (based on Fig. 1b):

$$\left.\frac{\partial c_+}{\partial x}\right|_{x=0} = 0,\ \left.\frac{\partial \phi_2}{\partial x}\right|_{x=0} = 0 \text{ at } x = 0 \text{ (at the separator electrode interface)} \tag{12}$$

$$c_+ = c_{+,2} \text{ and } \phi_2 = \phi^* \text{ at } x = L_2 \tag{13}$$

For the solid phase, they solved Eqs. (3), (4) and (7). The current transfer from the solid phase to the electrolyte was calculated from [91]

$$i_2(x) = -F\, D_s \left.\frac{\partial c_s}{\partial r}\right|_{r=R_s} \tag{14}$$

The authors assumed that the electrode and the electrolyte are initially in equilibrium, and used this assumption to calculate initial concentrations in both phases based on an equilibrium correlation. This is a pseudo two-dimensional model (r and x directions). They used finite difference methods to solve the equations described above numerically. Their model does not include the effect of the separator in the cell and uses a fixed boundary condition at $x = L_2$, when it would have been more appropriate to use the general flux boundary condition as Mao and White used [92]. West et al. [91] concluded that the electrolyte depletion is the principal limiting factor in the capacity obtained during the discharge of their system.

Mao and White [92] developed a mathematical model for a liquid organic electrolyte cell (Li/LiClO$_4$/TiS$_2$). Their schematic of the cell is similar to the one given in Fig. 1b, except that they did not include the tabs. They used dilute solution theory for their model. For the electrolyte phase in the electrode they used Eq. (11), they also used Eq. (11) for the electrolyte in the separator but without the term $i_2(x)$. Their boundary condition for $x = 0$ is given by Eq. (12). Mao and White [92] used a flux boundary condition at the interface between the separator and the positive electrode (Eq. (9) Ref. [92]). At the lithium-foil electrode they equated the flux of Li$^+$ to the dissolution rate of Li (Eq. 14 Ref. [92]). Mao and White [92] solve a pseudo two-dimensional system (r, x) using a finite difference method. They used a three point approximation for the dimensional variables (x, r) and the Crank Nicolson approximation for the temporal variable to obtain accuracy on the order of $(\Delta x)^2$and $(\Delta t)^2$. Their system of equations was solved using the algorithm developed by Mao and White [115]. The authors concluded that a porous TiS$_2$ electrode in a cell with thin separator would deliver much more capacity than the electrode would in a large volume of electrolyte, and that the utilization of the TiS$_2$ electrode increases with a decrease in the separator thickness [92]. Their analysis demonstrated the importance of including the separator in a battery model.

Doyle et al. [93] developed a mathematical model for a one-dimensional polymer electrolyte cell (Li/PEO$_8$–LiCF$_3$SO$_3$/TiS$_2$) using concentrated solution theory, where the driving force is the gradient of the chemical potential [2]. An investigation [116] of the mechanism of conduction in these electrolytes concluded that ion pairing and ion association interactions are important in these electrolytes. These kind of interactions can be included by using concentrated solution theory, while dilute solution theory only includes the interactions between the solute and the solvent [2]. However, it is important to note that many properties required by the concentrated solution theory have not been measured yet for the lithium battery systems (e.g. activity coefficients), and this is an important point for making the decision about the complexity of a model. The mass balance on the salt in the separator is given by [93]

$$\frac{\partial c}{\partial t} = \nabla\cdot\left[D(c)\left(1 - \frac{\mathrm{d}\ln(c_0)}{\mathrm{d}\ln(c)}\right)\nabla c\right] - \frac{i_2\cdot\nabla t^0_+(c)}{z_+ v_+ F} \tag{15}$$

The variation of the potential in the separator is calculated from [2]

$$i_2 = -\kappa(c)\,\nabla\phi_2 - \frac{\kappa(c)\,RT}{F}\left(1 + \frac{\partial \ln f_\pm}{\partial \ln c}\right)\left(\frac{s_+}{n\,v_+} + \frac{t^0_+(c)}{z_+\,v_+}\right)\nabla\ln(c) \tag{16}$$

The Butler–Volmer equation is used for the kinetic expression [2]. The material balance in the cathode is given by [93]

$$\varepsilon\frac{\partial c}{\partial t} = \nabla\cdot(\varepsilon D(c)\nabla c) - \frac{i_2\cdot\nabla t^0_+(c)}{z_+\,v_+\,\mathrm{F}} + \frac{a\,j_n(1 - t^0_+)}{v_+} \tag{17}$$

The pore wall flux (j_n) is related to the divergence of the current flow in the electrolyte phase through [93]

$$a\,j_n = -\frac{S_+}{n\,F}\nabla\cdot i_2 \tag{18}$$

Eqs. (15)–(17) illustrate the main difference of treating the system using concentrate solution theory, instead of using dilute solution theory in which Eqs. (10) and (11) apply [91,92]. Doyle et al. [93] used diffusion as the mechanism of transport of lithium in the solid phase as described by Eqs. (3)–(6). Since the equations describing this process are linear, their solution can be obtained using Duhamel's superposition integral for a step change in the surface concentration (Eqs. (B-1) to (B-6) Ref. [93]). This approach enabled Doyle et al. [93] to transform the pseudo two-dimensional problem (r, x) into a one-dimensional problem (x); therefore, the solution technique is much faster than the approach used in Refs. [91] and [92]. The disadvantage of this approach is that it does not allow including non-linearities in the solid phase such as the effect of the concentration in the solid on the diffusion coefficient in the solid phase, thus their method way may not be useful for cases where strong interactions are presented in the system as shown by Verbrugge and Koch [100].

More details about the equations required for the modeling of lithium/polymer battery systems can be found in the review prepared by Doyle and Newman [94]. Typically, Newman and his coworkers solve these equations by using the Crank–Nicolson method to evaluate the time derivatives together with the subroutine BAND [2] to solve the system of equations. At the interfaces between the separator and the electrodes, they use the subroutine BAND and the integration method (also called control volume formulation method). Botte et al. [44] have shown that the results obtained using Newman's technique for the interface are not as accurate as those obtained by using three point forward and three point backward approximations for the derivatives at the interface together with the subroutine MBAND [32].

Fuller et al. [84] extended the model by Doyle et al. [93] to simulate a lithium-ion cell. Their equations are very similar to those by Doyle et al. [93], except that the negative electrode is treated in the same way as the positive electrode (a material balance for the negative electrode is also given by Eq. (17)). The models by Doyle et al. [93] and Fuller et al. [84] have shown good agreement with experimental data [90,96,99].

Darling and Newman [97] modeled the behavior of a porous intercalation electrode with two characteristic particle sizes. Their equations are the same as those used by Doyle et al. [93], but they assumed constant properties and an ideal solution (i.e. the activity coefficient, $f_\pm = 1$). They wrote material balances for the two different particles size everywhere in the electrode. They generated a bimodal particle size distribution with the same mass of a uniform particle distribution using the following equation [97]

$$\frac{\varepsilon_1}{\varepsilon_p} = \frac{R_{s,2}/R_{s,u} - 1}{R_{s,2}/R_{s,1} - 1} \tag{19}$$

They observed that the coulombic capacity of the non-uniform electrodes was less than that of the uniform electrode at a given discharge rate during a galvanostatic discharge. This means that the capacity estimated using a uniform distribution might show poor agreement with the capacity of a real cell, especially at high discharge rates. They also observed that the non-uniform electrodes required more time to equilibrate than the uniform electrodes during a relaxation period. The significant effect of the non-uniformity of the electrode in the behavior of the battery indicates that non-uniformity of the particle sizes should be included in the model in order to obtain more realistic results, especially at high discharge rates. This approach is interesting, however, it is important to keep in mind that they assumed a constant mass for the active material (the mass of the electrode is the same for an uniform and non-uniform particle distribution). It may be also significant to determine the ratio of the particle sizes required to obtain a given porosity in the active material that would allow maximizing the capacity of the cell.

An approach like this was considered by Nagarajan et al. [56]. They developed a mathematical model to study the effect of the particle size distribution on the galvanostatic discharge behavior of a liquid organic electrolyte cell and/or polymer electrolyte cell. They used dilute solution theory and the same assumptions made by Mao and White [92]. Nagarajan et al. [56] used the linear packing model developed by Yu et al. [117] to account for the porosity of the electrode as a function of the mixture of particles of different sizes. They [56] considered a binary mixture of small and large particles, where the volume fractions of the small (x_S) and large (x_L) particles are known. The specific volume of the mixture is calculated based on the volume fraction of the particles and the specific volume for a random packing of spheres (V_o). The equation for the specific volume will depend on the array matrix [56]

$$V_L = V_o\,x_L + \hat{V}_S\,x_S \tag{20}$$

$$V_S = V_o\,x_S + \hat{V}_L\,x_L \tag{21}$$

Eq. (20) applies for a matrix of large particles where the voids are filled with small particles, while Eq. (21) applies for a matrix of small particles where the voids are filled with large particles. The specific volume of the mixture of particles is given by the maximum between V_S and V_L. The maximum was chosen to avoid overlapping of the particles. The other equations used to complete their model are given as Eqs. (23), (24), (26), and (27) of Ref. [56]. The derivatives in the differential equations were cast in finite difference forms for the spatial derivatives and were solved using the method of lines and the DASSL subroutine to solve over time. The code was written using the program FWEB [62]. They concluded [56] that a binary mixture can provide a significantly higher density of active material relative to an electrode comprised of single-size particles. However, increasing the packing density increases the liquid-phase diffusion resistance; therefore, there is an optimum size ratio for these variables to increase the capacity of the cell [56]. This analysis is important and should be combined with the thermal modeling of a cell (there will probably be a trade off between capacity and safety).

Another important factor to consider during the modeling of lithium batteries is the fade in capacity. None of the models that we have mentioned above incorporate capacity fade mechanisms. Arora et al. [118] presented a review of capacity fade mechanisms and side reactions in lithium-ion batteries. Doyle et al. [96] modified their dual lithium-ion model to include film resistances on both electrodes, and they determined the value of these resistances needed to fit experimental data for a lithium ion battery ($Li_xC_6/LiPF_6$,EC–DMC/$Li_yMn_2O_4$). These resistances will affect the values of the overpotential as shown in Eq. (11) of Ref. [96]. These film resistances are not capacity fade mechanisms but instead parameters used to fit experimental data, further work needs to be done to explain the origin of these film resistances. Doyle et al. [96] suggested that the resistances are described satisfactorily by either a film resistance on the electrode particles or by contact resistances between the cell layers.

Darling and Newman [98] were the first one to model a capacity fade mechanism by incorporating electrolyte decomposition in a Li/$LiClO_4$–PC, p(VdF-HFP)/$Li_yMn_2O_4$ cell. Their model enables one to predict the loss of capacity based on cell discharge. Recently, Arora et al. [101] developed a model to predict lithium deposition on the negative electrode under a variety of operating conditions. They used a $Li_xC_6/LiPF_6$-EC-DMC, p(VdF-HFP)/$LiMn_2O_4$ cell in the simulations. Their model can be used to establish operational and design limits within which the lithium deposition overcharge reaction can be avoided [101].

Capacity fade mechanisms probably depend on the system, the active materials used, the electrolyte, solvent, etc. In addition, it is likely that other capacity fade mechanisms exist and have not yet been identified. Modeling of the loss of capacity during cycling is an active area of research.

2.2. Thermal models

The thermal models developed for secondary lithium batteries are based on idealized conditions of the system. They [102–107] do not include the details associated with the cell sandwich shown in Fig. 1. Chen and Evans [102–104] developed two and three dimensional mathematical models to study the thermal behavior of a polymer electrolyte [102–104] and lithium ion [105] prismatic batteries. In their models the energy balance is given by [103,104]

$$\rho \ C_p \frac{\partial T}{\partial t} = k_x \frac{\partial^2 T}{\partial x^2} + k_y \frac{\partial^2 T}{\partial y^2} + k_z \frac{\partial^2 T}{\partial z^2} + q \tag{22}$$

The z dependence (third term on the r.h.s. of Eq. (22)) is neglected for the two-dimensional models (Refs. [102–104]). They assumed that the heat generation term is uniform through the cell for the solution of Eq. (22) and is given by [102–105]

$$q = \frac{N_{cell} \ I \left(U_{oc} - V - T\frac{d \, U_{oc}}{d \, T} \right)}{L} \tag{23}$$

In this approach the discharge and charge curves (I–V curves) need to be supplied. These discharge and charge curves can be measured for the system under consideration and can also be fitted by using Eqs. (9) and (21) of Ref. [119] during discharge and charge, respectively. One of the advantages of this approach is that Eq. (22) and the associated boundary conditions can be solved easily (the boundary conditions for the system will depend on the geometry, cooling system used, presence or lack of insulation, etc.). A disadvantage is that the study of the system is limited to the conditions under which the discharge and charge curves are measured. If the effect of variables such as: porosity of the materials, particle size, materials, electrolyte concentration, separator, etc., needs to be evaluated more experimental data is required (the discharge and charge curves would need to be measured for all of the changes in these variables).

Chen and Evans [102–105] solved Eq. (22) and its boundary (internal and external) and initial conditions (Eqs. (3)–(5) of Ref. [102]) using the finite difference method. The boundary conditions were treated by using the implicit alternating-direction technique [120]. Chen and Evans [102–104] studied the effect of variables such as: cell thickness, cooling system, and discharge rates in the thermal behavior of the batteries, and concluded that thermal management is not a serious problem for lithium polymer batteries at low discharge rates. The authors [105] also simulated the effect of thermal runaway in the battery by assuming a localized heat source similar to the that used by Evans and White [121]. This approach allows studying the effect of a localized heat source in the cell stack, but it does not allow determining the cause of the heat source. They [105] concluded that during normal battery operation, the battery does not reach the onset temperature for thermal runaway. However, if a battery is continuously cycled under high rate charge/discharge rate, significant heat can be generated in the battery.

Kanari et al. [106] used an approach similar to Chen and Evans [102–105] but they applied the energy balance in cylindrical coordinates, assuming temperature changes only in the radial and axial directions (Eq. (1) of Ref. [106]). The authors [106] modeled a C/Li_xCoO_2 cell and obtained good agreement with the experimental data. Neither, Chen and Evans [102–105] nor Kanari et al. [106] incorporated the effect of the temperature on the thermal properties (conductivity and specific heat).

Verbrugge [107] modeled the temperature and current distribution in a battery module for a lithium/polymer electrolyte/vanadium oxide cell. His model (three-dimensional) includes the assumption that no significant concentration gradients exist in the electrolyte, a linear relation exits (current-potential) for the electrochemical reactions, and only one electrochemical reaction occurs at the each electrodes. Verbrugge determined the potential distribution in the module by assuming that the potential gradient in the cell can be expressed as a series of resistances and is given by [107]

$$\frac{\partial V}{\partial x} = N\, U_{\mathrm{oc}} - \frac{I_x}{\sigma_x} \tag{24}$$

for the x direction and [107]

$$\frac{\partial V}{\partial y} = -\frac{I_y}{\sigma_y} \text{ and } \frac{\partial V}{\partial z} = -\frac{I_z}{\sigma_z} \tag{25}$$

for the y and z directions, respectively. The determined material charge conductivities are expressed as a series of resistances [107]

$$\frac{1}{\sigma_x} = N\left(\frac{L_1}{\sigma_1} + \frac{L_2}{\sigma_2} + \frac{L_s}{\sigma_s} + \frac{R\,T}{i_{o1} n\, F} + \frac{R\,T}{i_{o2} n\, F}\right) \tag{26}$$

$$\sigma_y = \sigma_z = \frac{L_1}{L}\sigma_1 + \frac{L_2}{L}\sigma_2 + \frac{L_s}{L}\sigma_s \tag{27}$$

Eqs. (24) and (25) were solved simultaneously with the energy balance in the battery. An energy balance expressed for an isobaric battery system as given by Bernardi et al. [9]

$$Q = I_{\mathrm{app}}\left(V + \frac{\Delta H}{nF}\right) + M\, C_{\mathrm{p}}\frac{\mathrm{d}T}{\mathrm{d}t} \tag{28}$$

The combination of the energy balance with the potential distribution is summarized in Eq. (18) of Ref. [107]. This equation was solved using the finite difference method. Verbrugge [107] expressed the heat capacities, densities and thermal conductivities of the materials as a function of the temperature. His approach (series of resistances) allows a mathematical representation of the system in three dimensions, however, effect of variables such as: particle size of the electrodes, concentration of the electrolyte, high discharge rates, were not included.

Pals and Newman [108] developed a one-dimensional mathematical model to predict the thermal behavior of a lithium/polymer cell. In their model they assumed that the temperature is constant through the cell but changes with time. They extended Doyle's one-dimensional model [93] to obtain the temperature of the cell by solving the energy balance as shown by Bernardi et al. [9]

$$I\left(U_{\mathrm{oc}} - V - T\frac{\mathrm{d}U_{\mathrm{oc}}}{\mathrm{d}T}\right) = h_{\mathrm{s}}(T - T_{\mathrm{a}}) + M_{\mathrm{a}}\, C_{\mathrm{p}}\frac{\mathrm{d}T}{\mathrm{d}t} \tag{29}$$

Therefore, current and voltage values are obtained from the solution of the macroscopic mass balance. The authors [108] analyzed the behavior of the cell for isothermal conditions, and different values of the heat transfer coefficient including adiabatic condition ($h_s = 0$).

Pals and Newman [109] developed a cell stack model to predict the temperature profiles in cell stacks based on the isothermal results of a one-dimensional cell obtained in Ref. [108]. They [109] used heat generation rates from isothermal discharges to estimate the heat generation rates during non-isothermal discharges. This approach is an approximation that allows an easier mathematical solution of the system; however, the exact solution can only be obtained by solving the mass and energy balances simultaneously.

Botte et al. [11] studied the influence of some design variables (current density, porosity of the electrodes, particle size of the electrodes, thickness of the electrodes, etc.) in the thermal behavior of a lithium ion cell based on a one dimensional mathematical model. Their model is based on the one-dimensional model developed by Fuller et al. [84] The authors [11] modified the energy balance described by Rao and Newman [10] to incorporate the effect of the decomposition reaction of the negative electrode in the thermal behavior of the cell. The decomposition reaction of the negative electrode is modeled as describe by von Sacken [122]

$$\Re = k_1 a_4 \bar{c}_{\mathrm{s},1} \exp\left(\frac{-E_{\mathrm{A}}}{RT}\right) \tag{30}$$

A complete derivation of the energy balance for the system is presented [11] and the final results are summarized by Eq. (8) of Ref. [11]. The authors concluded that a more accurate estimation of the parameters used to describe the decomposition reaction of the negative electrode is necessary to improve the predictions of their model [11]. This approach is an attempt to study the effect of side reactions in the thermal behavior of a lithium ion cell.

All of these workers [11,108,109] assumed that the transport properties are independent of temperature.

They solved the mass balance of the system at a given temperature and evaluated the temperature of the cell based on the results of the material balance. None of them solved the mass and energy balance simultaneously.

3. Conclusions

The insertion (and de-insertion) process in a porous lithium electrode has mostly been modeled as a diffusion process assuming the concentration gradient as the driving force with constant solid diffusion coefficient. Only Verbrugge and Koch [100] proposed to use the gradient of the chemical potential as the driving forced for this process in the solid state. It appears that their procedure is better, but it would be valuable to determine whether or not it is necessary. We would also like to suggest that more work is need to describe quantitatively the thermodynamics of the solid phase in cathode materials. First principles calculations and molecular dynamics can be very useful for doing this. The work by Verbrugge and Koch [100] on this topic for lithium ion intercalation into carbon should be done for cathode materials. The modeling of these systems depends critically on the quantitative representation of the open circuit potential as a function of the concentration of lithium ion in the solid state. No one has modeled a complete secondary lithium cell including material and energy balance simultaneously in more than one dimension, due to the complexity of the system. Such a model would help us understand the lithium battery system better and may provide insight into the thermal runaway issue. None of the models has incorporated a mechanism that is able to predict thermal runaway in secondary lithium batteries and this is basically because this phenomenon is not yet understood. The trend is to incorporate capacity fade mechanisms in the modeling of secondary lithium batteries and to predict their cycling behavior. For doing this, the fade capacity mechanisms need to be understood and it may take some years of research before these mechanisms can be quantified and incorporated into models. Molecular simulations may help understand these mechanisms.

Appendix A. List of symbols

a	specific interfacial area of solid-phase particles per unit volume of porous electrode (m^2/m^3)
a_4	ratio of the solid volume of the anode insertion material to volume of cell sandwich (m^3/m^3)
$\bar{c}_{s,1}$	average surface concentration of Li^+ in solid phase of the anode (mol/m^3)
c	concentration of electrolyte (mol/m^3)
c_0	concentration of solvent (mol/m^3)
c_-	concentration of anions in the electrolyte (mol/m^3)
c_+	concentration of Li^+ in the electrolyte (mol/m^3)
$c_{+,2}$	concentration of Li^+ in the electrolyte just outside the pores (mol/m^3)
c_s	concentration of Li^+ inside an electrode particle (mol/m^3)
c_s^*	surface concentration of Li^+ in an electrode particle (mol/m^3)
c_t	maximum or saturation concentration of Li^+ in the solid phase (mol/m^3)
C_p	constant pressure battery or cell heat capacity, (J/kg per K)
D	diffusion coefficient of the electrolyte (m^2/s)
D_-	diffusion coefficient of anions in the electrolyte (m^2/s)
D_+	diffusion coefficient of Li^+ in the electrolyte (m^2/s)
D_I	diffusion coefficient of infinitely dilute Li^+ in the solid electrode (m^2/s)
D_s	diffusion coefficient of Li^+ in the solid electrode particles (m^2/s)
E_A	activation energy for the decomposition reaction of the anode (Eq. (30)), (J/mol)
F	characteristic constant of the electrode material (Eq. (7)), dimensionless
$f_\pm$	activity coefficient, dimensionless
F	Faraday's constant (96487 C/mol)
G	specific surface area per unit volume (1/m)
G^E	excess free energy (J/mol)
h_s	heat transfer coefficient (W/m^2 per K)
I	superficial current density (A/m^2)
I_{app}	applied current in the cell or battery (A)
i_2	current density at particle-electrolyte interface (A/m^2)
i_{o1}	exchange current density in the anode (A/m^2)
i_{o2}	exchange current density in the cathode (A/m^2)
j_n	pore wall flux of Li^+ at the surface of the electrode particle (mol/m^2 per s)

k_1	anode decomposition reaction rate constant (1/s)
k_x	average thermal conductivity in the x direction (W/m per K)
k_y	average thermal conductivity in the y direction (W/m per K)
k_z	average thermal conductivity in the z direction (W/m per K)
L	thickness of cell or cell stack (m)
L_1	thickness of the anode (m)
L_2	thickness of the cathode (m)
L_c	thickness of the current collector (m)
L_e	thickness of the electrode (m)
L_s	thickness of the separator (or the electrolyte in a polymer cell) (m)
L_t	thickness of the tab (m)
M	mass of the cell or battery (kg)
M_a	mass of the cell or battery per unit area (kg/m^2)
n	number of electrons transferred in the electrode reaction given in Eq. (1), dimensionless ($n = 1$)
N	cell number in a stack per unit length x (1/m)
N_{cell}	number of cells in a stack
q	rate of heat generation per unit volume of the battery or cell (W/m^3)
Q	rate of heat transfer into the battery from the surroundings (W)
r	radial coordinate of electrode particles (m)
R	universal gas constant (8.3143 J/mol per K)
R_s	electrode particle diameter (m)
$\mathfrak{R}$	anode decomposition rate of reaction per volume of the cell (Eq. (30)), (mol/m^3 per s)
s_+	stoichiometric coefficient of cations involved in the general insertion process given in Eq. (1), dimensionless ($s_+ = 1$)
S_s	ratio of diffusion time to discharge time, dimensionless
t	time (s)
t_+^0	transference number of cations, dimensionless
T	temperature of the cell (K)
T_a	ambient temperature (K)
U_{oc}	open circuit potential of the cell (V)
V	battery or cell potential (V)
$V(\tau)$	time dependent function used in the Appendix
V_L	specific volume when large particles are the controlling component, dimensionless
V_o	specific volume for a packing of spheres, dimensionless (Eqs. (20) and (21))
V_s	specific volume when small particles are the controlling component, dimensionless
$\hat{V}_L$	partial specific volume of the large particles, dimensionless
$\hat{V}_S$	partial specific volume of the small particles, dimensionless
x	spatial coordinate of cell sandwich (m)
x_L	volume fraction of large component, dimensionless
x_S	volume fraction of small component, dimensionless
y	spatial coordinate of cell sandwich (m)
z	spatial coordinate of cell sandwich (m)
z_+	charge of cations in the electrode reaction given in Eq. (1), dimensionless ($z_+ = 1$)

Greek letters

ΔH	enthalpy of the reaction (J/mol)
ε	porosity of the electrode, dimensionless
ϕ_1	potential in solid phase (V)
ϕ_2	potential in electrolyte phase (V)
ϕ^*	potential in electrolyte phase just outside the pore (V)
$(\phi_1 - \phi_2)^{\theta}$	characteristic constant of the electrode material (V)
γ_I	activity coefficient of Li$^+$ in the solid phase, dimensionless
κ	ionic conductivity of the electrolyte (S/m)
ν_+	number of cations into which a mole of electrolyte dissociates, dimensionless
Ω_k	self interaction coefficient of order k (J/mol)
ρ	battery or cell density (kg/m^3)
σ_1	charge conductivity in the anode (S/m)
σ_2	charge conductivity in the cathode (S/m)
σ_s	charge conductivity in the separator (or electrolyte in a polymer cell) (S/m)
σ_x	charge conductivity in the x direction (S/m)
σ_y	charge conductivity in the y direction (S/m)
σ_z	charge conductivity in the z direction (S/m)

θ_I	fractional occupancy of Li^+, dimensionless
θ_s	site in the solid insertion material
Superscripts	
0	initial time condition ($t = 0$)
1	specie 1 or negative electrode
2	specie 2 or positive electrode
u	uniform
p	active material particles
Subscripts	
k	order of the series given in Eq. (9), dimensionless

References

[1] R.B. Bird, W.E. Stewart, E.N. Lightfoot, Transport Phenomena, Wiley, New York, 1960.
[2] J.S. Newman, Electrochemical Systems, Englewood Cliffs, New Jersey, 1991.
[3] J.S. Newman, W. Tiedemann, AIChE J. 21 (1975) 25.
[4] J.S. Dunning, Ph.D. Thesis, University of California, Los Angeles, 1971.
[5] J.S. Trainham, Ph.D. Thesis, University of California, Los Angeles, 1979.
[6] P. De Vidts, R.E. White, J. Electrochem. Soc. 144 (1997) 1343.
[7] J.A. Prins-Jansen, J.D. Fehribach, K. Hemmes, J.H.W. de Wit, J. Electrochem. Soc. 143 (1996) 1617.
[8] C.Y. Wang, W.B. Gu, B.Y. Liaw, J. Electrochem. Soc. 145 (1998) 3407.
[9] D. Bernardi, E. Pawlikowski, J. Newman, J. Electrochem. Soc. 132 (1985) 5.
[10] L. Rao, J. Newman, J. Electrochem. Soc. 144 (1997) 2697.
[11] G.G. Botte, B.A. Johnson, R.E. White, J. Electrochem. Soc. 146 (1999) 914.
[12] M. Jain, J.W. Weidner, J. Electrochem. Soc. 146 (1999) 1370.
[13] H.S. Carslaw, J.C. Jaeger, Conduction of Heat in Solids, Oxford University Press, London, 1993, p. 242.
[14] J. Crank, Mathematics of Diffusion, Oxford University Press, London, 1994.
[15] P.G. Ciarlet, J.L. Lions, Handbook of Numerical Analysis, vol. I, Elsevier, New York, 1990, p. 3.
[16] M.E. Davis, Numerical Methods and Modeling for Chemical Engineers, Wiley, New York, 1984, p. 75.
[17] C. Pozrikidis, Numerical Computation in Science and Engineering, Oxford University Press, New York, 1998, p. 482.
[18] C. Pozrikidis, Introduction to Theoretical and Computational Fluid Dynamics, Oxford University, New York, 1997, p. 558.
[19] P. De Vidts, R.E. White, Computers Chem. Eng. 16 (1987) 1007.
[20] B.S. Haran, R.E. White, Computer Applications in Engineering Education 4 (1996) 229.
[21] V.R. Subramanian, R.E. White, A semi-analytical method for predicting current and potential distributions, on tutorials, in: R.F. Savinell, A.C. West (Eds.), Electrochemical Engineering, The Electrochemical Society, Pennington, NJ, 1999.
[22] V.R. Subramanian, R.E. White, J. Electrochem. Soc., 1999 (in press).
[23] R.E. White, Ind. Eng. Chem. Fundam. 17 (1978) 369.
[24] J. Van Zee, M.A. Edmund, R.E. White, Ind. Eng. Chem. Fundam. 19 (1980) 438.
[25] T.V. Nguyen, R.E. White, Computers Chem. Eng. 11 (1987) 543.
[26] P.S. Fedkiw, Eng. 6 (1982) 327.
[27] D.A. Curtis, T.I. Evans, R.E. White, J. Electrochem. Soc. 136 (1989) 3392.
[28] H.A. Preisig, R.E. White, Comput. Chem. Engng. 14 (1990) 179.
[29] M. Matlosz, J. Newman, Comput. Chem. Eng. 11 (1987) 45.
[30] J. Van Zee, G. Kleine, R.E. White, J. Newman, in: R.E. White (Ed.), Electrochemical Cell Design, Plenum Press, New York, 1984.
[31] M.C. Kimble, R.E. White, Comput. Chem. Engng. 14 (1990) 921.
[32] D. Fan, R.E. White, J. Electrochem. Soc. 138 (1991) 1688.
[33] D. Fan, R.E. White, Comput. Chem. Engng. 15 (1991) 797.
[34] Z. Mao, R.E. White, J. Electrochem. Soc. 141 (1994) 151.
[35] S. Patankar, Numerical Heat Transfer and Fluid Flow, Hemisphere Publishing Corporation, New York, Hemisphere Publishing, New York, 1980, p. 31.
[36] A. West, T. Fuller, J. Appl. Electrochem. 26 (1996) 557.
[37] R.S. Varga, Matrix Iterative Analysis, Prentice-Hall, Englewood Cliffs, New Jersey, 1965, p. 161.
[38] R.H. Stark, J. Assoc. Comput. Mach. 3 (1956) 29.
[39] A.N. Tikhonov, A.A. Samarskii, Doklady Akad. Nauk SSSR (N.S.) 108 (1956) 393.
[40] R.S. Varga, IRE Trans. of the Professional Group on Nuclear Science NS-4, (1958) 52.
[41] E.L. Wachspress, in: A. Ralston and H.S. Wilf (Eds.), The Numerical Solution of Boundary Value Problems, Wiley, New York, 1960.
[42] G.I. Marchuk, Numerical Methods for Nuclear Reactor Calculations, Consultants Bureau, New York, 1959, p. 293.
[43] H.K. Versteeg, W. Malalasekera, An Introduction to Computational Fluid Dynamics. The Finite Volume Method, Longman Group, Malaysia, 1995.
[44] G.G. Botte, J.A. Ritter, R.E. White, Comput. Chem. Eng., 1999 (submitted).
[45] G.G. Botte, R.E. White, Computers Chem. Eng., 1999 (submitted).
[46] P.M. Gresho, R.L. Sani, Incompressible Flow and the Finite Element Method, Wiley, UK, 1998, p. 6.
[47] A. Varma, M. Morbidelli, Mathematical Methods in Chemical Engineering, Oxford, New York, 1997, p. 56.
[48] V.R. Subramanian, B.S. Haran, R.E. White, Computers Chem. Eng. 23 (1999) 287.
[49] C.L. Smith, R.W. Pike, P.W. Murill, Formulation and Optimization of Mathematical Models, International Textbook Company, Pennsylvania, 1970, p. 381.

[50] V.R. Subramanian, R.E. White, Comput. Chem. Eng., 1999 (submitted).
[51] Mathcad7, User's Guide, MathSoft, Inc., Cambridge, 1997.
[52] J. Glynn, T. Gray, The Beginners Guide to Mathematica version 3, Cambridge, New York, 1997.
[53] C. de Boor, A Practical Guide to Splines, Springer-Verlag, New York, 1978.
[54] PDE/PROTRAN, A System for the Solution of Partial Differential Equations, IMSL, Inc., 1989.
[55] FLUENT CFD, http://www.fluent.com/applicat/applicat.htm
[56] G.S. Nagarajan, J.W. Van Zee, R.M. Spotnitz, J. Electrochem. Soc. 145 (1998) 771.
[57] P. De Vidts, R.E. White, J. Electrochem. Soc. 142 (1995) 1509.
[58] P. De Vidts, J. Delgado, R.E. White, J. Electrochem. Soc. 143 (1996) 3223.
[59] P. De Vidts, J. Delgado, B. Wu, D. See, K. Kosanovich, R.E. White, J. Electrochem. Soc. 145 (1998) 3874.
[60] Y. Zhang, H.Y. Cheh, J. Electrochem. Soc. 146 (1999) 850.
[61] H.P. Langtangen, Computational Partial Differential Equations, Numerical Methods and Diffpack Programming, Springer-Verlag, New York, 1999.
[62] D.E. Knuth, Literate Programming, Standford University, CA, 1992.
[63] R. Compton, http://physchem.ox.ac.uk:8000/frame.shtml
[64] L.K. Bieniasz, Towards Computational Electrochemistry – a Kineticist's Perspective, to be published in Modern Aspects of Electrochemistry, J.OM. Bockris, B.E. Conway, R.E. White (Eds.), Plenum Press, New York.
[65] Y. Ma, M. Doyle, T.F. Fuller, M.M. Doeff, L.C. De Jonghe, J.S. Newman, J. Electrochem. Soc. 142 (1859) 1995.
[66] X.G. Sun, Y.Q. Lin, L.M. Ding, X.B. Jing, Electrochim. Acta 41 (1996) 1573.
[67] U.V. Alpen, M.F. Bell, Electrochemical Properties of some Solid Lithium Electrolytes, P. Vashishta, J.N. Mundy, G.K. Shenoy (Eds.), Elsevier North Holland, Inc., 1979.
[68] J. Barker, R. Pynenburg, R. Koksbang, M.Y. Saidi, Electrochim. Acta 41 (1996) 2841.
[69] J.M. Sullivan, D.C. Hanson, R. Keller, J. Electrochem. Soc. 117 (1970) 779.
[70] A.L. de Oliveira, O. Damasceno, P.R. Silva, C.L. Sangiorge, J.P. Donoso, T.J. Bonagamba, Electrochim. Acta 42 (1997) 929.
[71] P. Yu, B. Popov, J. Ritter, R.E. White, J. Electrochem. Soc. 146 (1999) 8.
[72] M.W. Verbrugge, B.J. Koch, J. Electrochem. Soc. 146 (1999) 833.
[73] M. Doyle, Ph.D. Thesis, University of California, Berkeley, 1995.
[74] J.-S. Hong, H. Maleki, S. Al Hallaj, L. Redey, J.R. Selman, J. Electrochem. Soc. 145 (1998) 1489.
[75] H. Maleki, S. Al Hallaj, J.R. Selman, R.B. Dinwiddie, H. Wang, J. Electrochem. Soc. 146 (1999) 947.
[76] M.E. Garcia, S.H. Garofalini, J. Electrochem. Soc. 146 (1999) 696.
[77] I.A. Courtney, J.S. Tse, O. Mao, J. Hafner, J.R. Dahn, Phys. Rev. B 58 (1998) 15583.
[78] G. Nuspl, M. Nagaoka, K. Yoshizawa, F. Mohri, T. Yamabe, Bull. Chem. Soc. Japan 71 (1998) 2259.
[79] A. Marquez, A. Vargas, P.B. Balbuena, J. Electrochem. Soc. 145 (1998) 3328.
[80] J. Soetens, C. Millot, B. Maigret, J. Phys. Chem. A 102/7 (1998) 1055.
[81] R.J. Blint, J. Electrochem. Soc. 142 (1995) 696.
[82] J.N. Reimers, J. Power Sources 54 (1995) 16.
[83] S. Hossain, in: D. Linden (Ed.), Handbook of Batteries, McGraw-Hill, New York, 1995.
[84] T.F. Fuller, M. Doyle, J. Newman, J. Electrochem. Soc. 141 (1994) 1.
[85] S. Atlung, K. West, T. Jacobsen, J. Electrochem. Soc. 126 (1979) 1311.
[86] M. Doyle, J. Newman, J. Appl. Electrochem. 27 (1997) 846.
[87] M. Doyle, J. Newman, J. Power Sources 54 (1995) 46.
[88] S. Atlung, B. Zachau-Christiansen, K. West, T. Jacobsen, J. Electrochem. Soc. 131 (1984) 1200.
[89] R. Darling, J. Newman, J. Electrochem. Soc. 144 (1997) 3057.
[90] T.F. Fuller, M. Doyle, J. Newman, J. Electrochem. Soc. 141 (1994) 982.
[91] K. West, T. Jacobsen, S. Atlung, J. Electrochem. Soc. 120 (1982) 1480.
[92] Z. Mao, R.E. White, J. Power Sources 43/44 (1993) 181.
[93] M. Doyle, T.F. Fuller, J. Newman, J. Electrochem. Soc. 140 (1993) 1526.
[94] M. Doyle, J. Newman, Electrochim. Acta 40 (1995) 2191.
[95] M.W. Verbrugge, B.J. Koch, J. Electrochem. Soc. 143 (1996) 24.
[96] M. Doyle, J. Newman, J. Electrochem. Soc. 143 (1890) 1996.
[97] R. Darling, J. Newman, J. Electrochem. Soc. 144 (1997) 4201.
[98] R. Darling, J. Newman, J. Electrochem. Soc. 145 (1998) 990.
[99] P. Arora, M. Doyle, A.S. Gozdz, R.E. White, J. Newman, In: J.W. Van Zee and T.F. Fuller (Eds.), Comparison between Computer Simulations and Experimental Data for High-Rate Discharges of Plastic Lithium-Ion Batteries, Proceedings of the 194th ECS Conference, Boston, 1998.
[100] M.W. Verbrugge, B.J. Koch, J. Electrochem. Soc. 143 (1996) 600.
[101] P. Arora, M. Doyle, R.E. White, J. Electrochem. Soc., 2000 (in press).
[102] Y. Chen, J.W. Evans, J. Electrochem. Soc. 140 (1833) 1993.
[103] Y. Chen, J.W. Evans, Electrochim. Acta 39 (1994) 517.
[104] Y. Chen, J.W. Evans, J. Electrochem. Soc. 141 (1994) 2947.
[105] Y. Chen, J.W. Evans, J. Electrochem. Soc. 143 (1996) 2708.
[106] K. Kanari, K. Takano, Y. Saito, T. Masuda, Thermal Simulation of Spiral Wound Cylindrical Type Lithium Batteries, Proceedings of International Workshop on Advanced Batteries, Osaka, 1995.

[107] M.W. Verbrugge, AIChE J. 41 (1995) 1550.

[108] C.R. Pals, J. Newman, J. Electrochem. Soc. 142 (1995) 3274.

[109] C.R. Pals, J. Newman, J. Electrochem. Soc. 142 (1995) 3282.

[110] V.R. Subramanian, R.E. White, Separation of Variables for Diffusion in Composite Electrodes with Flux Boundary Conditions, in: R.F. Savinell, A.C. West (Ed.), Tutorials in Electrochemical Engineering, The Electrochemical Society, Inc., Pennington, New Jersey, 1999.

[111] B. Davies, B. Martin, J. Comput. Phys. 33 (1979) 1.

[112] D.G. Duffy, ACM Trans. Math. Software 19 (1993) 333.

[113] K. Wohl, Trans. AIChE 42 (1946) 215.

[114] I. Uchida, H. Fujiyoshi, S. Waki, J. Power Sources 68 (1997) 139.

[115] Z. Mao, R.E. White (unpublished program, available upon request).

[116] M.A. Ratner, In: J.R. MacCalumm, C.A. Vincent (Ed.), Polymer Electrolyte Reviews-1, Elsevier Applied Science, London, 1987.

[117] A.B. Yu, R.P. Zou, N. Standish, Ind. Eng. Chem. Res. 35 (1996) 3730.

[118] P. Arora, R.E. White, M. Doyle, J. Electrochem. Soc. 145 (1998) 3647.

[119] C.M. Shepherd, J. Electrochem. Soc. 112 (1965) 657.

[120] B. Carnahan, H.A. Luther, J.O. Wilkers, Applied Numerical Method, Wiley, New York, 1969, p. 452.

[121] T.I. Evans, R.E. White, J. Electrochem. Soc. 136 (1989) 2145.

[122] U. von Sacken, Nodwell, E. Sundher, J.R. Dahn, Solid State Ionics 69 (1994) 284.